Development of an analytical model for predicting the wet collapse pressure of curved flexible risers

Li, X.; Jiang, Xiaoli; Hopman, Hans

DOI
10.1016/j.oceaneng.2021.109132

Publication date
2021

Document Version
Final published version

Published in
Ocean Engineering

Ocean Engineering 232 (2021) 109132

Contents lists available at ScienceDirect

Ocean Engineering

journal homepage: www.elsevier.com/locate/oceaneng

Development of an analytical model for predicting the wet collapse pressure of curved flexible risers

Xiao Li *, Xiaoli Jiang, Hans Hopman

Department of Maritime and Transport Technology, Delft University of Technology, Netherlands

ARTICLE INFO

Keywords:
Flexible pipes
Curvature effect
Collapse behaviors
Wet collapse
Analytical solution

ABSTRACT

Flexible risers are designed with strong anti-collapse capacities which enable them to operate in deep-water reservoirs. However, this anti-collapse capacity is susceptible to the pipe curvature in the flooded annulus condition. For the curved riser sections within the touch-down zone, significant reduction of collapse capacity can occur once their external sheaths are worn out by the seabed, resulting in the so-called "wet collapse". Mostly, wet collapse studies of curved flexible risers are performed through costly numerical simulations since there are no alternative analytical approaches. In view of it, this work presents an analytical model for predicting the wet collapse pressure of curved flexible risers. The analytical model is developed based on a spring-supported arch model that from our previous work, which is able to take the curvature-induced factors into account. With the stability theories of arched structures, the wet collapse pressure of curved flexible risers can be solved. To verify this analytical model, 3D full FE models are employed. The critical collapse pressures predicted by these two kinds of approach are in good agreement, indicating this proposed analytical model can be an useful tool to facilitate the collapse analysis in pipe design stage.

1. Introduction

Flexible risers are widely used in offshore production to convey hydrocarbons from sub-sea reservoirs to floating vessels. They are multi-layered tubular structures which consist of helical wound metal bands and extruded thermoplastics (Rahmati et al., 2016), as shown in Fig. 1 (Weppenaar and Andersen, 2014). Owing to their internal helical structural layout, they can tolerant large bending deformation and be used in different riser configurations (Brouard et al., 2016; Simpson and Lima, 2019). This makes the flexible riser a key device in deep-water production (Clarke et al., 2011; Lukassen et al., 2019).

As nowadays hydrocarbon production moves to the reservoirs in water depth of 3000 m (Murawski et al., 2020), flexible risers have to withstand huge hydro-static pressure without collapse. To predict and design the collapse strength of those tubular structures accurately, studies regarding their collapse capacity have been carried out extensively to understand all the possible influential factors like installation loads, curvature, material hardening as well as radial gaps (Miyazaki et al., 2018; Caleyron et al., 2017; Skjerve et al., 2014; Axelsson and Skjerve, 2014; Deng et al., 2016; Lin et al., 2016; Deng et al., 2019). Even so, the collapse failure of flexible risers is still an issue that have not been fully addressed.

Collapse failure of flexible risers caused by hydro-static pressure is commonly divided into two types, dry and wet collapse, depending on the annulus conditions of flexible risers (API, 2014a; Gay Neto and Martins, 2012). Dry collapse may occur when the outer sheath is intact and all layers within the riser play a role together to resist the hydro-static pressure. Once the outer sheath is breached, as shown in Fig. 2 (Crome, 2013; Mahé, 2015), the seawater floods the riser annulus and the external pressure acts directly on the inner sheath. This situation, named wet collapse, represents the most extreme loading condition since the whole external pressure is resisted by the carcass alone. Other layers, mainly the pressure armor, contributes to the collapse resistance by restraining the radial deformation of the carcass.

At present, the collapse capacity of a flexible riser is designed based on the "wet collapse" concept (API, 2014a,b), which makes the collapse capacity of flexible risers to be designed conservatively. However, it was found that the wet collapse resistance is susceptible to the pipe curvature. Curved collapse tests done by companies such as TechnipFMC (Technip) (Paumier et al., 2009) and BHGE (Wellstream) (Lu et al., 2008; Clevelario et al., 2010) showed that the wet collapse pressure could be reduced around 10%–20% when the pipe samples were bent to their minimum bending radius (MBR) (API, 2014b). Therefore, the curvature effect cannot be ignored in the wet collapse analysis of flexible risers.

Curved collapse calculations, for the most part, are performed by numerical simulations since they allow better insight into the structural

* Corresponding author.
E-mail address: X.Li-9@tudelft.nl (X. Li).

https://doi.org/10.1016/j.oceaneng.2021.109132
Received 25 December 2020; Received in revised form 19 April 2021; Accepted 25 April 2021
Available online 11 May 2021

Nomenclature

α	Half of the included angle of the arch
β	Half of the included angle of the detached carcass
Δ_0^c	Initial ovalization of the bent pipe
Δ_0	Initial ovalization of the straight pipe
Δ_{ad}	Additional ovalization
κ	Pipe curvature
ω	Radial deflection
ρ	Arch radius
σ_y	Yielding stress
σ_θ	Hoop stress
τ	Angle enclosed by the differential element
θ	Angle for the arbitrary section AA' of the arch
υ	Poisson's ratio
ξ	Angle measured from neutral plane to section AA'
A	Cross-sectional area
C	Correction factor of the rectangular cross section in shear
$C_1 - C_3, D_1 - D_8, K$	Coefficients
E	Young's Modulus
F	Radial compression force
G	Shear modulus
I	Inertia moment
k_t	Combined elastic stiffness of the pressure armor and the liner
L	Pitch
M	Bending moment
N	Hoop force
N_0, M_0	Reaction force and bending moment at the section on the neutral plane
N_{thrust}	Hoop thrust force at the arch ends
P_s	Harmonic squeeze load
q	Uniform radial load
Q_x	Radial shear force
R	Radius
R_s	Distance between the separation point to the carcass center
U	Strain energy
u, w	Radial and circumferential displacements

Subscripts

c	Properties of the carcass
cr	Properties related to the collapse moment
eq	Equivalent properties of the carcass
ex	Properties related to the carcass extrados
l	Properties of the liner

Superscripts

,	$\frac{\partial}{\partial\theta}$

integrity and layer interaction, as shown in Fig. 3. Due to the structural complexity of flexible pipes, however, the modeling and the computation in numerical simulations are always time-consuming (Gay Neto et al., 2012). By contrast, analytical models are more convenient in early stages of design. For the collapse analysis, most of analytical

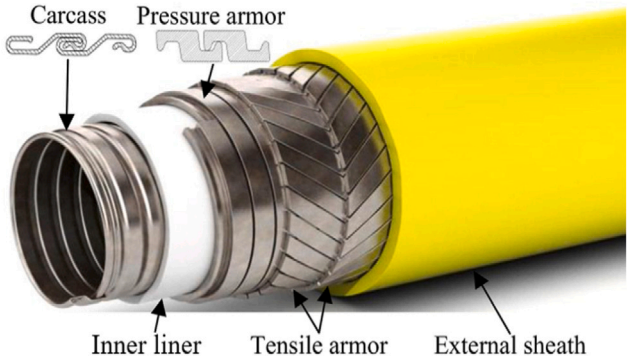

Fig. 1. Typical configuration of a flexible riser (Weppenaar and Andersen, 2014).

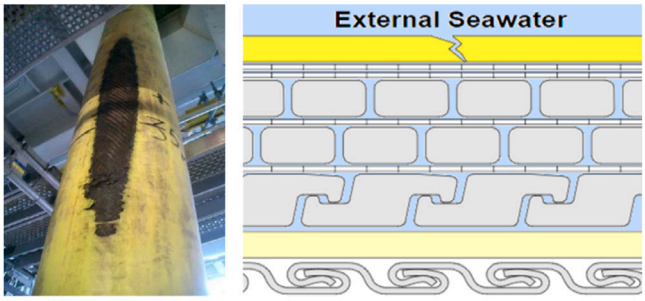

Fig. 2. Flooded annulus scenario for the flexible riser with a breached outer sheath (Crome, 2013; Mahé, 2015).

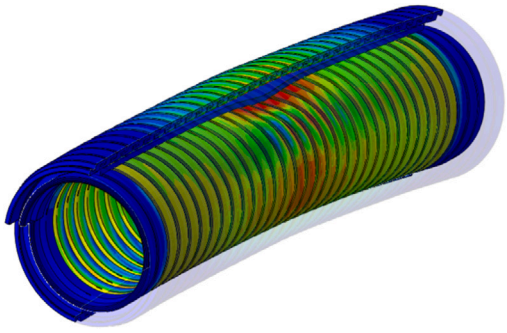

Fig. 3. Finite element model for collapse analysis.

models are developed from a general ring buckling model presented by Timoshenko and Gere (Timoshenko and Gere, 1963). Various equivalent layer methods have been proposed to treat the interlocking layers as equivalent homogeneous rings (Martins et al., 2003; Li et al., 2018a,b). With this treatment, those analytical models simplify the flexible pipe as a concentric ring structure, solving the collapse pressure based on the buckling theories of rings. Mostly, those analytical models are used to predict the collapse pressure of straight risers (Glock, 1977; Bai et al., 2016). The main difficulty of using analytical models in curved collapse is how to address the global curvature effect with a two-dimensional ring model.

In such a context, this work presents an analytical model to address the curved wet collapse issue of flexible risers, which aims to facilitate the collapse calculations in the pipe design stage. Prior to this work, a mechanism study (Li et al., 2020a) was conducted by our team to gain insight into the wet collapse behaviors of curved flexible risers. This study reveals that the curvature effect for reducing the wet collapse resistance of flexible risers is the result of three factors: the squeeze-induced additional ovalization, the pitch elongation and the deformed

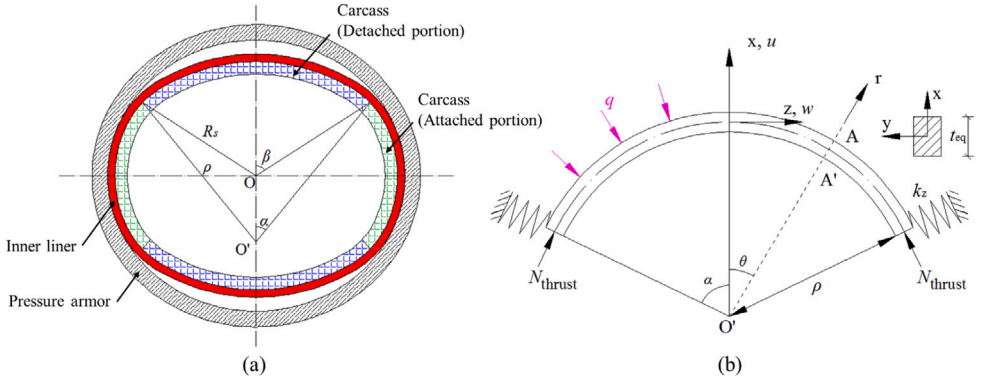

Fig. 4. A spring-supported arch model for the detached portion of the carcass under uniform radial pressure (Li et al., 2020b).

cross-sectional shape of the carcass. Among them, the deformed cross-sectional shape of the carcass is the major contributing factor to the curvature effect. Following that mechanism study, an analytical model is developed in this work to predict the wet collapse pressure of curved risers, which is able to take those three factors into account.

In our previous work (Li et al., 2020b), a spring-supported arch model was proposed to predict the wet collapse pressure for straight flexible risers with initial ovalization and inter-layer gap. The arch model is taken as a theoretical framework in this paper to incorporate the curvature effect. The rest of the paper is organized as follows: in Section 2, the arch model is first briefly outlined, followed by the model development to incorporate the above-mentioned three factors. Section 3 presents the verification of the analytical model, in which the 3D full FE models from our previous mechanism study (Li et al., 2020a) are employed. Discussions based on the results from both the analytical and numerical models are given in Section 4. The conclusions are given in the final section.

2. Model development

In order to predict the wet collapse pressure of curved flexible risers, a spring-supported arch model from our previous work (Li et al., 2020b) was used. This arch model was proposed for wet collapse analysis of straight risers, which is regarded as a theoretical framework in this study to incorporate curvature effect for the curved collapse issue. The whole model development is going to be described with two subsections. The first subsection briefly outlines the theoretical framework for the collapse analysis while the second subsection clarifies how to introduce the curvature-induced factors into this framework.

2.1. Theoretical framework

For the flexible riser with a breached outer sheath, the hydro-static pressure is mainly withstood by the innermost carcass. In this situation, the carcass is buckled under the external pressure, with a deformation as illustrated in Fig. 4(a). Since wet collapse is governed by the buckling strength of the detached portions of the carcass, simplification can be made in the theoretical analysis to regard those portions as a circular arch with a new center O', as shown in Fig. 4(b). In this figure, r-θ-y is the cylindrical coordinate system whose origin locates at the arch center O'; x–y–z is the local Cartesian coordinate system of the arch cross section.

As the radial deformation of the carcass is restrained in the contact regions, the surrounded pressure armor together with the liner is treated as springs that supports at the arch ends. Therefore, a spring-supported arch model was proposed to predict the wet collapse pressure of straight flexible pipes. By using the equivalent layer methods (Martins et al., 2003; Li et al., 2018a), such an arch can be built with equivalent wall thickness and material properties.

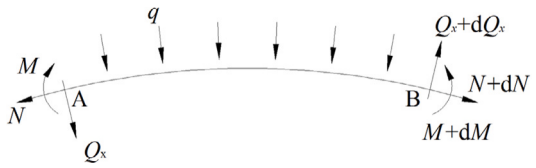

Fig. 5. Equilibrium of a differential element of the arch.

To solve the buckling pressure of this spring-supported arch, one assumption given by Timoshenko and Gere (1963) is adopted, which assumes that the carcass collapses when its maximum hoop compressive stress reaches the material yield stress. With this assumption, the wet collapse pressure can be determined by equating the maximum hoop compressive stress of the arch to its material equivalent yield stress. For the circular arch subjected to uniform radial pressure, the general linear equilibrium equation set for its differential element can be expressed as (Tong, 2005)

$$\begin{cases} Q_x' - N - q\rho = 0 \\ N' + Q_x = 0 \\ M' + Q_x\rho = 0 \end{cases} \tag{1}$$

where M, N, and Q_x are the bending moment, hoop force and radial shear force on the differential element, the positive directions of those internal forces are shown in Fig. 5; ρ is the arch radius; superscript $'$ represents $\frac{\partial}{\partial\theta}$; θ is the angle for an arbitrary section AA' of the arch; q is the uniform loads along the radial direction. Using displacements to reformulate Eqs. (1), then

$$\begin{cases} E_{eq}A_{eq}\frac{w''+u'}{\rho} = 0 \\ E_{eq}A_{eq}\frac{w'+u}{\rho} + \frac{E_{eq}I_{eq}}{\rho^3}(u^{IV} + 2u'' + u) = -\rho q \end{cases} \tag{2}$$

where u and w, as shown in Fig. 4(b), are displacements of the differential element along the radial and circumferential directions, separately; E denotes the Young's Modulus; A denotes the cross-sectional area; I is the inertia moment and R is the radius; the items with subscript 'eq' refer to the equivalent properties of the carcass for the arch. If taking K as

$$K = -\frac{\rho^3}{E_{eq}I_{eq}}(\rho q + E_{eq}A_{eq}\frac{w'+u}{\rho}) \tag{3}$$

Then the general solution of Eqs. (2) can be written as

$$\begin{cases} u = KC_1\cos\theta + KC_2\theta\sin\theta + K \\ w = -KC_1\sin\theta - KC_2(\sin\theta - \theta\cos\theta) + KC_3\theta \end{cases} \tag{4}$$

where $C_1 \sim C_3$ are constants that determined by the boundary conditions. The internal forces at any cross section, defined by the angle θ,

are

$$\begin{cases} N = \frac{E_{eq}A_{eq}K}{\rho}(1+C_3) + \frac{E_{eq}I_{eq}K}{\rho^3}(1+2C_2\cos\theta) \\ M = \frac{E_{eq}I_{eq}K}{\rho^2}(2C_2\cos\theta+1) \\ Q_x = \frac{E_{eq}I_{eq}K}{\rho^3}(2C_2\sin\theta) \end{cases} \tag{5}$$

For a spring-supported arch model as depicted in Fig. 4(b), it has boundary conditions at its arch ends as

$$\begin{cases} w|_{\theta=\alpha} = 0, & \text{No hoop displacement} \\ N|_{\theta=\alpha} = N_{\text{thrust}}, & \text{Force equilibrium in hoop direction} \\ (Q_x + k_t u)|_{\theta=\alpha} = 0, & \text{Force equilibrium in radial direction} \end{cases} \tag{6}$$

where N_{thrust} is the hoop thrust force at the arch end; α is the half of the included angle of the circular arch; k_t is the elastic stiffness of the pressure armor together with the liner. With the above boundary conditions, the formulae of $C_1 \sim C_3$ can be derived.

By substituting the coefficients into Eqs. (5), the maximum compressive stress at the crown point of the arch can be written as a function of the external pressure q. Since the wet collapse is defined by material yielding, therefore, the collapse pressure q_{cr} of the arch can be worked out as

$$\sigma_{y,eq} + \sigma_\theta(q_{cr})|_{\theta=0} = \sigma_{y,eq} + \frac{N_{cr}}{t_{eq}} - \frac{6M_{cr}}{t_{eq}^2} = 0 \tag{7}$$

where σ_y is the material yielding stress; σ_θ is the hoop stress; t denotes the wall thickness; subscript 'cr' represents the parameters at the moment of collapse.

2.2. Curvature-induced factors

In our previous mechanism study (Li et al., 2020a), three factors induced by pipe curvature can lead to the decrease of wet collapse resistance, which are the deformed cross-sectional shape and the pitch elongation of the carcass, and the squeeze effect of the liner. The first two factors affect the collapse modes while the third one impose an additional ovalization onto the carcass. In what follows, these factors are introduced to the theoretical framework step by step.

2.2.1. Cross-sectional shape of the carcass

The geometry of the circular arch is directly related to the deformed cross-sectional shape of the carcass under external pressure. Depending on the initial ovalization types and pipe curvature of flexible pipes, the carcass could collapse into symmetrical, bi-symmetrical or transitional shapes (Li et al., 2020b). Compared to the bi-symmetrical oval-shaped carcass, a symmetrical one leads to a circular arch with a smaller rise-span ratio, providing less collapse resistance to the hydro-static pressure. In this work, the carcass with singly and doubly initial ovalization is studied respectively, as depicted by the section CC' in Fig. 6. In order to provide a conservative prediction of the wet collapse, the singly ovalization in this study is always introduced to the side of the carcass where pitch elongation occurs during the bending.

Considering a carcass with a doubly initial ovalization first, as shown in Fig. 7. The collapse mode of this initial doubly-ovalized carcass gradually turns from a bi-symmetrical shape to a symmetrical one with the increase of pipe curvature. Assuming the circumference of the carcass remains unchanged during the collapse process, then the arch radius ρ and included angle 2α can be determined based on the cross-sectional shapes as below.

$$\text{Bi}-\text{symmetrical} \quad \begin{cases} 2\pi R_c - 2R_s(\pi - 2\beta) = 4\alpha\rho \\ \rho\sin\alpha = R_s\sin\beta \end{cases} \tag{8}$$

$$\text{Symmetrical} \quad \begin{cases} 2\pi R_c - 2R_s(\pi - \beta) = 2\alpha\rho \\ \rho\sin\alpha = R_s\sin\beta \end{cases} \tag{9}$$

where R_s is the distance from the separation point to the ring center at the collapse moment, and β is the corresponding angular quantity

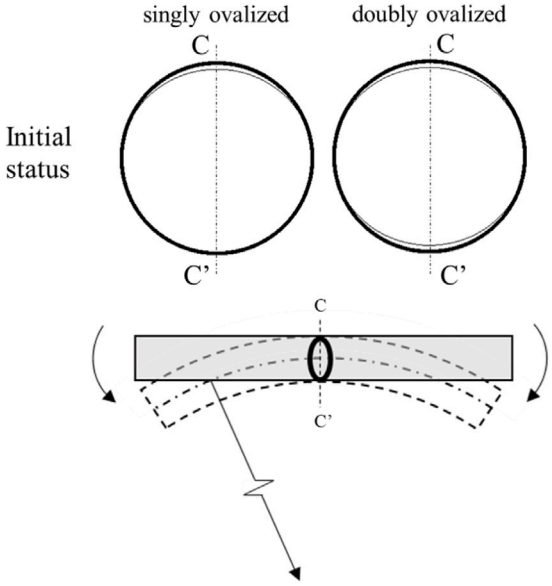

Fig. 6. Singly and doubly initial ovalization.

displayed in Fig. 7, they can be calculated by referring to our previous work (Li et al., 2020b); the items with subscript 'c' refer to the properties of the carcass. In this doubly initial ovalized case, the bi-symmetrical shape is adopted in the wet collapse prediction of straight risers while the symmetrical one is used for the risers bent to their MBR. The collapse pressures from these two pipe configurations are regarded as upper and lower bounds in the wet collapse analysis. Based on these two bounds, the wet collapse pressure of risers with a curvature in-between can be predicted by interpolation.

For the carcass with a singly initial ovalization, its cross section is assumed to perform a symmetrical shape at the collapse moment, no matter the pipe is in a straight or curved configuration. Therefore, the formulas of the symmetrical shape can be used to determine the arch geometry for the riser with a singly initial-ovalized carcass. By substituting the arch radius and angle into the corresponding equations listed in the theoretical framework, this curvature-induced shape effect is included.

2.2.2. Pitch elongation

The pitch of the carcass extrados is elongated during the bending, as shown in Fig. 8. This pitch elongation reduces the superposed areas between two carcass profiles within one pitch, making the carcass extrados less stiff and easier to be collapsed. In our theoretical framework, the carcass extrados is treated as an equivalent arch. By determining the equivalent properties of the carcass extrados, the reduced radial stiffness caused by the pitch elongation is introduced into the arch model.

For the flexible riser bent with a curvature of κ, the elongated pitch of the carcass extrados is given as (Sævik and Ye, 2016).

$$L_{c,ex} = L_c(R_c\kappa + 1) \tag{10}$$

where $L_{c,ex}$ is the elongated pitch of the carcass extrados; L_c is the carcass pitch of a straight riser without any external loads; κ represents the pipe curvature. With the elongated pitch from Eq. (10), equivalent properties of the carcass extrados can be determined for the arch model. A strain energy-based equivalent method presented in our previous work (Li et al., 2018a) is adopted in this arch model, which builds the equivalences between the carcass and its equivalent layer with their membrane stiffness, and the absorbed strain energy. The strain energy is obtained by subjecting the carcass and its equivalent layer to a radial compression force that could cause the onset of material yielding of the

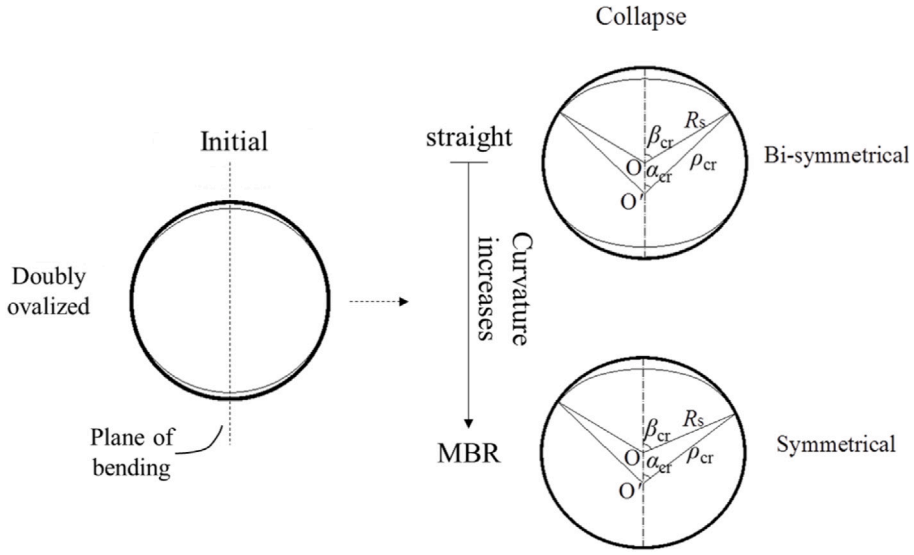

Fig. 7. Collapse mode of initial doubly-ovalized carcass influenced by the pipe curvature.

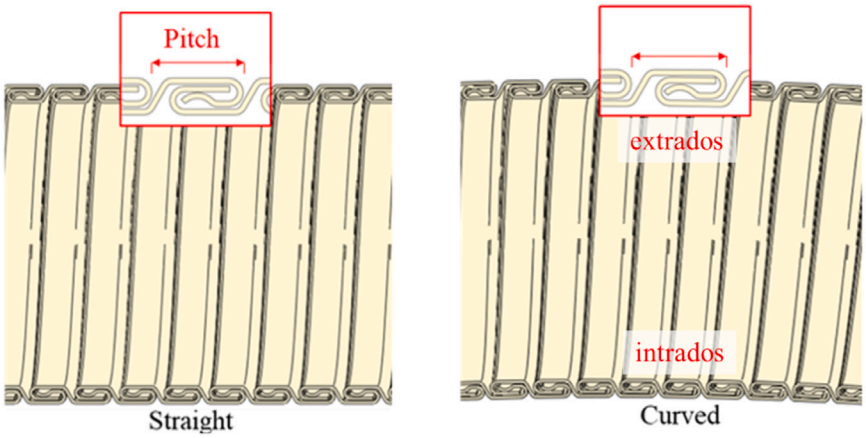

Fig. 8. Pitch elongation on the carcass extrados due to bending.

carcass. With this strain energy-based method, the equivalent thickness and Young's Modulus of the carcass can be determined by

$$\begin{cases} U_c = U_{eq} = \frac{F^2 R_c (1-\upsilon_c^2)}{32}\left[\frac{\pi}{A_{eq}E_{eq}} + \frac{C\pi}{A_{eq}G_c} + \frac{12R_c^2(\pi^2-8)}{E_{eq}t_{eq}^3 L_{c,ex}\pi}\right] \\ E_c\frac{A_c}{L_{c,ex}} = E_{eq}t_{eq} \end{cases} \tag{11}$$

where U_c and U_{eq} are the strain energy of the carcass and its equivalent layer; F is the radial compression force for triggering the onset of material yielding of the carcass; υ is the Poisson's ratio; C is the correction factor for a rectangular cross section in shear (Langhaar, 1962), and G is material shear modulus. The equivalent yield stress can be also worked out as

$$\sigma_{y,eq} = \sqrt{\frac{E_{eq}\sigma_y^2}{E_c}\frac{A_c}{L_{c,ex}t_{eq}}} \tag{12}$$

With Eqs. (11) & (12), the equivalent properties of the carcass extrados are determined for the arch. It should be noted that the strain energy-based equivalent layer method used here is just one way to involve the reduction effect of radial stiffness caused by the pitch elongation. Other equivalent methods such as bending stiffness equivalence per length (Martins et al., 2003) or per area (J.R.M. et al., 2001) could also be used as alternatives.

2.2.3. Squeeze effect of the liner

Owing to the large lay angle and interlocked nature of the carcass, the flexural stress introduced by bending can be neglected. However, the flexural stresses in the polymeric liner can generate a flattening load P_s to squeeze the cross section of the carcass (Sævik and Ye, 2016), as depicted in Fig. 9(a) (Gresnigt, 1986). For the flexible riser bent with a curvature of κ, the squeeze pressure generated by the liner can be calculated as (Brazier, 1927; Guarracino, 2003)

$$P_s(\xi) = \kappa^2 E_l t_l R_l \sin\xi \tag{13}$$

where P_s is the harmonic squeeze load; the items with subscript 'l' refer to the properties of the liner; ξ is the angle measured from neutral plane to section AA', as illustrated in Fig. 9(b). Under this squeeze load, the moment equilibrium at the section AA' of the carcass gives

$$M(\xi) = M_0 - N_0 R_c(1-\cos\xi) + R_c^2\int_0^{\xi} P_s(\xi)(\cos\tau - \cos\xi)\mathrm{d}\tau \tag{14}$$

where $\mathrm{d}\tau$ denotes the angle enclosed by the differential element; M_0 and N_0 are the bending moment and reaction force at the section that on the neutral plane, respectively. The reaction force N_0 can be derived as

$$\begin{aligned} N_0 &= \int_0^{\frac{\pi}{2}} P_s(\xi)R_c\sin\xi\mathrm{d}\xi \\ &= \frac{\pi}{4}\kappa^2 E_l t_l R_l R_c \end{aligned} \tag{15}$$

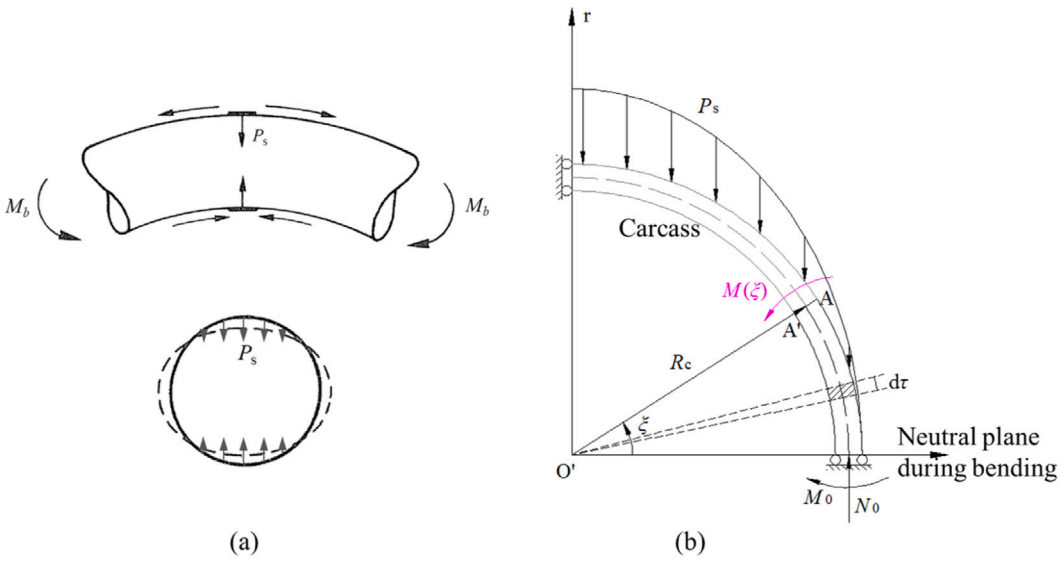

Fig. 9. (a) Squeeze load generated from the bent liner (Gresnigt, 1986) (b) Carcass ovalized under the squeeze load.

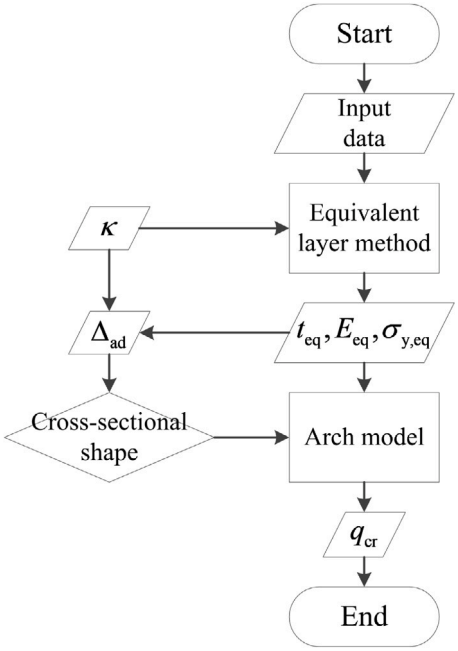

Fig. 10. Flowchart for the curved collapse analysis with the spring-supported arch model.

The bending moment M_0 can be also derived based on the Moment-area theorem

$$\int_0^{\frac{\pi}{2}} \frac{M(\xi)}{E_c I_c} R_c d\xi = 0 \tag{16}$$

$$M_0 = (\frac{2}{\pi} + \frac{\pi - 5}{4})\kappa^2 E_l t_l R_l R_c^2 \tag{17}$$

Thus, Eq. (14) can be written as

$$M(\xi) = \frac{1}{4}[\cos 2\xi + (\pi - 4)\cos\xi + \frac{8}{\pi} - 2]\kappa^2 E_l t_l R_l R_c^2 \tag{18}$$

Since the differential equation of radial deflection of the carcass is expressed as

$$\frac{d^2\omega}{d\xi^2} + \omega = -\frac{M(\xi)R_c^2}{E_{eq} I_{eq}} \tag{19}$$

where ω is the radial deflection caused by squeeze load P_s. With the conditions given below,

$$\frac{d\omega}{d\xi}\Big|_{\xi=0} = \frac{d\omega}{d\xi}\Big|_{\xi=\frac{\pi}{2}} = 0 \tag{20}$$

the radial deflection at the arbitrary section of the carcass takes form as

$$\omega(\xi) = \frac{\kappa^2 E_l t_l R_l R_c^4}{4 E_{eq} I_{eq}}[2 - \frac{8}{\pi} + \frac{\cos 2\xi}{3} + \frac{(4-\pi)(\xi \sin\xi + \cos\xi)}{2}] \tag{21}$$

Considering the pipe collapse is a plane strain issue, then the radial deflection of the carcass at ξ=0 and $\frac{\pi}{2}$ can be obtained as

$$\omega(0) = (1 + \frac{3\pi}{2} - \frac{24}{\pi})\frac{\kappa^2 E_l t_l R_l R_c^4}{E_{eq} t_{eq}^3}\frac{1 - \upsilon_c^2}{1 - \upsilon_l^2} \tag{22}$$

$$\omega(\frac{\pi}{2}) = (5 - \frac{3\pi^2}{4} + 3\pi - \frac{24}{\pi})\frac{\kappa^2 E_l t_l R_l R_c^4}{E_{eq} t_{eq}^3}\frac{1 - \upsilon_c^2}{1 - \upsilon_l^2} \tag{23}$$

Therefore, the additional ovalization caused by squeeze load is worked out as

$$\Delta_{ad} = \frac{\omega(\frac{\pi}{2}) - \omega(0)}{2R_c + \omega(\frac{\pi}{2}) + \omega(0)} \tag{24}$$

where Δ_{ad} is the additional ovalization due to the squeeze effect. For the straight riser with an initial ovalization Δ_0, it performs an ovalization for its curved configuration as

$$\Delta_0^c = \Delta_0 + \Delta_{ad} \tag{25}$$

where Δ_0 is the initial ovalization of the straight riser; Δ_0^c is the ovalization after bending. Δ_0^c can be regarded as a new initial ovalization for the spring-supported arch model (Loureiro and Pasqualino, 2012). Besides, additional hoop stresses in the carcass are also triggered by the applied squeeze load. At the crown point of the arch, the maximum compressive hoop stress caused by the squeeze load can be calculated as

$$\sigma_{\theta,ad}|_{\theta=0} = \frac{6M(\xi)|_{\xi=\frac{\pi}{2}}}{t_{eq}^2} \tag{26}$$

With this additional hoop stress, Eq. (7) is then improved as

$$\sigma_{y,eq} + \sigma_\theta(q_{cr})|_{\theta=0} + \sigma_{\theta,ad}|_{\theta=0} = 0 \tag{27}$$

By obtaining the new initial ovalization Δ_0^c as well as the additional hoop stress, the curvature-induced squeeze effect is included in this

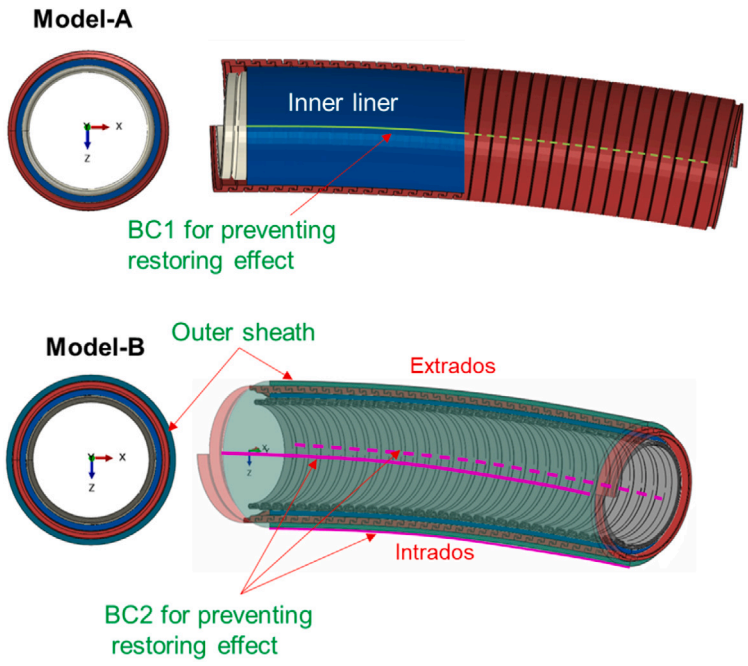

Fig. 11. Finite element models from the mechanism study: Model-A and Model-B (Li et al., 2020a).

arch model. With these three factors involved in the theoretical framework, the curvature effect is therefore considered in the wet collapse analysis. Below is a flowchart (see Fig. 10) which shows the whole prediction procedure of using this arch model. In the next section, case studies are conducted to verify this analytical model.

3. Model verification

The above section clarifies the development of the analytical model for incorporating the curvature effect. To verify this analytical model, the finite element models presented in our previous mechanism study (Li et al., 2020a) were employed. Case studies regarding various pipe curvature were carried out in this verification, in which the wet collapse pressures were predicted for the carcass with singly and doubly initial ovalization, respectively.

3.1. Doubly initial ovalization

In our previous study (Li et al., 2020a), two FE models, Model-A and Model-B, were established to study the wet collapse resistance of a 4" internal diameter (ID) bent flexible pipe that with a 0.5% doubly initial ovalization, as shown in Fig. 11. The detailed geometrical and material properties of this 4" pipe can be referred to the work of Gay Neto and Martins (2012, 2014). Model-A was a three-layer model with the carcass, the inner liner and the pressure armor. A boundary condition called BC1 was adopted in Model-A to prevent the restoring effect in curved collapse analyses, which was the nodes on the two lines of inner liner that were only allowed to move along X-axis direction after bending.

The BC1 was then found that had an interference on the collapse behavior of the carcass during the finite element studies. Therefore, Model-B was developed with an additional outer sheath, and BC2 replaced BC1 by moving the fixed lines to the outer surface of the outer sheath. The difference between these two FE models is the cross-sectional shape effect is excluded in Model-A due to the improper condition BC1 it adopted for preventing pipe restoration. Both these FE models were employed to verify the analytical model. Model-B was used to examine the reliability of the arch model in predicting the wet collapse pressure of curved risers. With the aid of Model-A, whether those curvature-induced factor were correctly considered in the arch model can also be examined.

Table 1
Equivalent properties of the carcass extrados for each radius of curvature.

Curvature radius (m)	Equivalent thickness (mm)	Equivalent Young's Modulus (GPa)	Equivalent yield stress (MPa)
∞	4.5	158.0	473.0
7	4.5	156.8	470.5
6	4.5	156.6	469.9
5	4.5	156.4	469.1
4	4.5	156.0	467.9
3	4.5	155.3	465.8

Table 2
Numerical and analytical results of pitch elongation and ovalization for each radius of curvature.

Curvature radius (m)		∞	7	6	5	4	3
Carcass Pitch (m)	FEA	16.00	16.14	16.16	16.20	16.25	16.32
	Analyt.	16.00	16.12	16.14	16.17	16.21	16.29
Ovalization after Bending (%)	FEA	0.500	0.509	0.510	0.511	0.515	0.523
	Analyt.	0.500	0.502	0.503	0.505	0.507	0.513

The case studies were conducted with a set of radius of curvature, which were 3 m (MBR), 4 m, 5 m, 6 m, 7 m, and ∞ (straight). By using the strain energy-based equivalent method, the equivalent properties for the analytical model in each curved case were work out as Table 1. Before the curved collapse analysis, a comparison was made between the analytical and numerical calculations regarding the pitch elongation and ovalization, which was given in Table 2. The aim of the comparisons is to show whether these two factors can be correctly estimated by the analytical formulations. It can be seen that both numerical and analytical calculations perform an increase of the same magnitude for each factor when the curvature goes up. Therefore, the analytical calculations of these two curvature-induced factors can be reliable inputs for the following curved collapse analysis.

With the equivalent properties and additional ovalization, the wet collapse pressures for different curvature were predicted by the analytical model. Although multiple factors were involved in the curvature effect, the cross-sectional shape of the carcass was identified by the

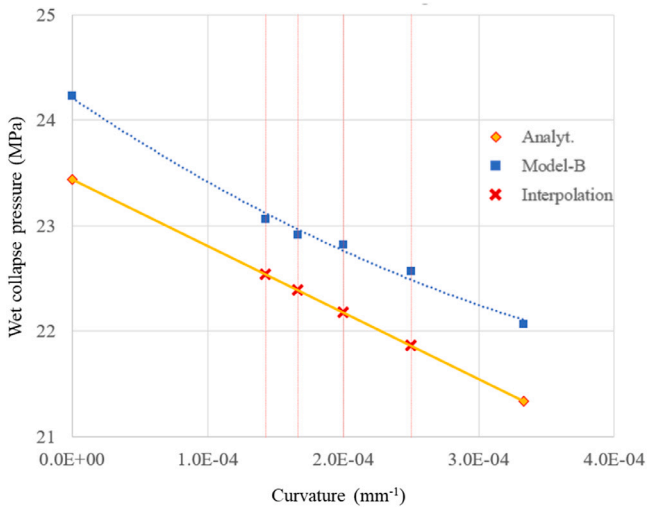

Fig. 12. Wet collapse pressure predicted by Model-B and the arch model for the risers with doubly initial ovalization.

Table 3
Comparison of wet collapse pressure between Model-A and the analytical model for no shape effect included.

Radius of curvature (m)		∞	7	6	5	4	3
Collapse Pressure (MPa)	Model-A	24.21	24.07	24.05	24.04	24.01	23.92
	Analyt.	23.44	23.26	23.22	23.18	23.12	23.01
Error (%)		3.20	3.39	3.44	3.57	3.71	3.80

Table 4
Comparison of wet collapse pressure between Model-B and the analytical model for doubly initial ovalization.

Radius of curvature (m)		∞	7	6	5	4	3
Collapse Pressure (MPa)	Model-B	24.23	23.06	22.91	22.82	22.57	22.07
	Analyt.	23.44	22.54	22.39	22.18	21.86	21.33
Error (%)		3.26	2.26	2.27	2.81	3.13	3.35

mechanism study as a major contributing factor to the reduction of the wet collapse strength. This should also be reflected by the analytical model. In this respect, Model-A and Model-B were used separately to verify the arch model with and without the incorporation of the shape factor. As the doubly initial-ovalized carcass within Model-A always performed an approximate bi-symmetrical cross section due to BC1, therefore, the bi-symmetrical shape was adopted in the corresponding arch model. Table 3 gives the wet collapse pressures predicted by Model-A and the arch model for no shape effect incorporated, which are in good agreement.

Model-B was employed to verify the arch model that incorporated all the curvature-induced factors. As stated in Section 2, the riser curved with a curvature less than MBR^{-1} presents a transition shape between the bi-symmetrical and symmetrical ones. This brings barriers to the prediction of the wet collapse pressure for those risers which are not heavily bent. To tackle this problem, a solution is proposed as follow. During the analytical prediction, the bi-symmetrical shape is adopted in the wet collapse prediction of straight risers while the symmetrical one is used for the risers in MBR. Based on the pressures from these two pipe configurations, the wet collapse pressures for the risers with transitions shape can be interpolated linearly according to their curvature.

Fig. 12 plots the collapse pressure given by Model-B and the analytical model for each curvature. With the above-mentioned solution, the wet collapse pressure for cases with a radius of curvature from 4 – 7 m were interpolated. Those data are listed in Table 4, which show a good correlation between the analytical and numerical predictions.

Table 5
Comparison of wet collapse pressure between Model-B and the analytical model for singly initial ovalization.

Radius of curvature (m)		∞	7	6	5	4	3
Collapse pressure (MPa)	Model-B	22.50	21.49	21.40	21.15	20.93	20.92
	Analyt.	20.81	20.68	20.65	20.62	20.56	20.46
Error (%)		7.50	3.77	3.49	2.52	1.74	2.16

3.2. Singly initial ovalization

The analytical model was further verified for predicting the wet collapse pressure of the curved risers which were singly initial ovalized. For comparative purposes, a singly initial ovalization of 0.5% was imposed to the carcass extrados side of Model-B, as shown in Fig. 13. By conducting the same curvature cases, this verification was made. For the riser with such a singly initial ovalization, the arch model assumes that it always triggers a symmetrical shape of the carcass at the collapse moment. Therefore, wet collapse pressures of all the cases predicted by the arch model were performed based on this symmetrical shape assumption, regardless of the pipe curvature. The predictions from the singly initial-ovalized Model-B and the arch model are listed in Table 5. It can be seen that the result from the arch model for each pipe curvature is in good agreement with numerical one, which shows a maximum error that less than 8%.

4. Result analysis and discussions

In Section 3, the analytical model is verified by the 3D full finite element models for both singly and doubly initial ovalization. According to our previous mechanism study (Li et al., 2020a), multiple factors such as pitch elongation and squeeze-induced ovalization are involved in the curvature effect. Among them, the deformed cross-sectional shape of the carcass is the one which contributes the most to the reduction of curved wet collapse resistance. To make sure whether this phenomenon could also be reflected by the analytical model, both FE Model-A and Model-B were employed in the verification.

Model-A was used to verify the analytical model which only incorporates the pitch elongation and the squeeze effect. According to Table 3, the analytical prediction of wet collapse pressure for each curvature case gives an error around 3.5% by comparing to the results of Model-A, indicating that these two factors are well considered in the analytical model. Furthermore, both the analytical and numerical results perform insignificant reduction of the wet collapse pressure with the increase of curvature radius from ∞ to 3 m, which are 1.83% and 1.2%, respectively. It implies that the effects of pitch elongation and squeeze-induced ovalization on the reduction of wet collapse resistance are limited.

By including the shape effect, the analytical model was then verified by Model-B for different initial ovalization types. For the doubly initial ovalization, the analytical model gives predictions of wet collapse pressure that correlate well with the numerical ones, with an error of 3% on average. This comparison shows that the analytical model is capable of predicting the wet collapse pressure of curved risers with doubly initial ovalization. Moreover, both of these two models show significant decreases of the wet collapse pressure with the increase of pipe curvature, which go up to 9% in the 3m case. This indicates that the shape effect does play an important role in the reduction of wet collapse resistance of curved flexible risers. Fig. 14 shows the deformed cross section of the doubly initial-ovalized carcass at the collapse moment for each pipe curvature.

For the singly initial ovalization, the predictions from the analytical model also agree well with the numerical results. In the curved cases, the differences between two kinds of prediction are less than 4%. However, the analytical model gives a much conservative prediction for the straight riser by comparing to Model-B. This is due to the fact

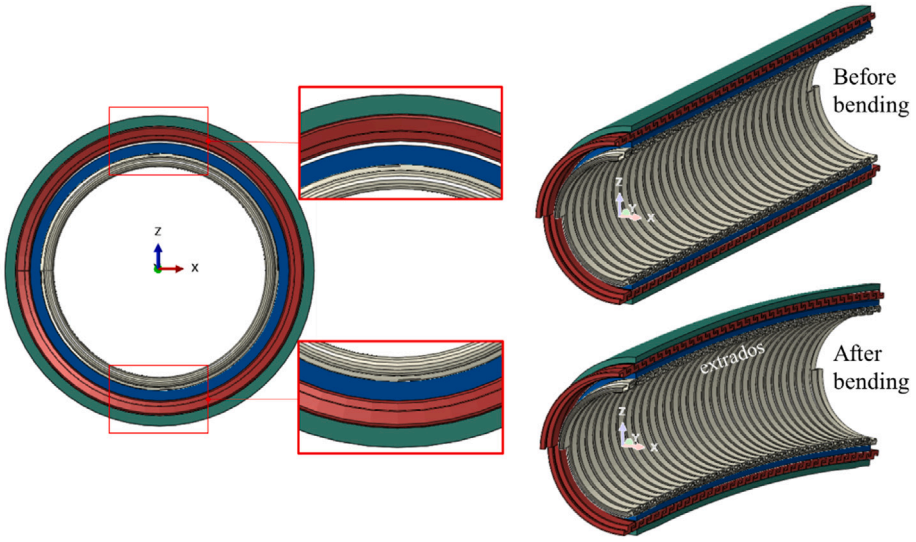

Fig. 13. Model-B with singly initial ovalization on its carcass extrados.

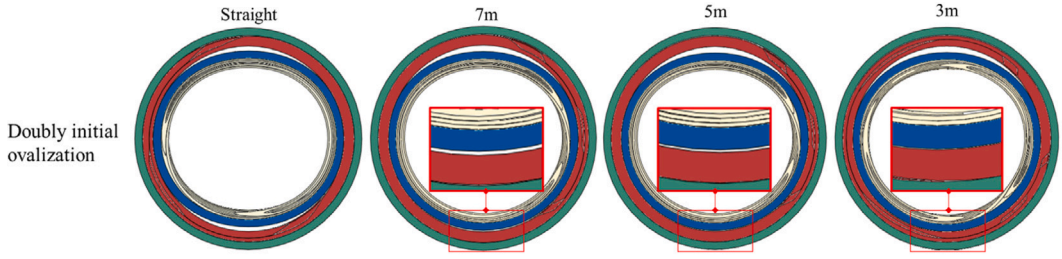

Fig. 14. View cut — cross-sectional shapes of the doubly initial-ovalized carcass at the collapse moment for different radius of curvature.

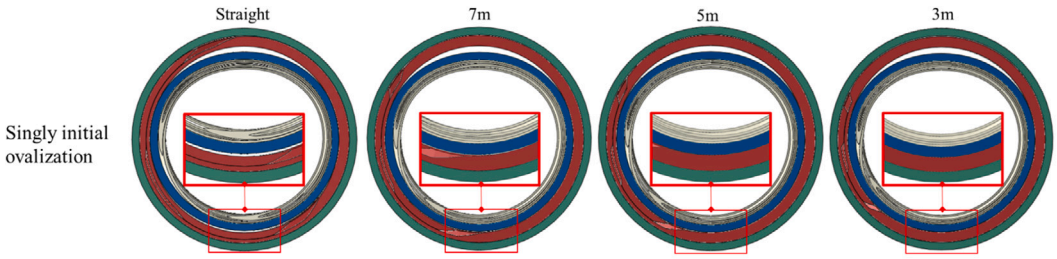

Fig. 15. View cut — cross-sectional shapes of the singly initial-ovalized carcass at the collapse moment for different radius of curvature.

that the applied external pressure can trigger a radial deflection of not only the (initial) ovalized portion but also the (initial) unovalized one, as shown in Fig. 13. Since ovalized and unovalized portions of the carcass have the closest radial stiffnesses for the riser in a straight configuration, a small deflection on the unovalized side could also be caused by the external pressure before the collapse of the ovalized portion. As a result, the straight case performs a transition shape rather than a symmetrical shape.

With the increase of curvature, the difference of radial stiffness between these two portions goes up. The external pressure is unable to cause a significant radial deflection of the unovalized portion before the final collapse. From the 7m case displayed in Fig. 15, an unclosed gap on the pipe intrados at the collapse moment could still be observed. When the radius of curvature goes above 5 m, there is no gap any more on the pipe intrados for the collapse moment. Since a symmetrical shape assumption is adopted in the analytical model for the singly initial-ovalized carcass, the wet collapse pressure is therefore conservatively predicted for the straight riser.

It should be noted that the deformed shapes of the carcass at the collapse moment do not represent the “heart” or “eight” mode in the post-buckling phase (Li et al., 2020b). For example, a bi-symmetrical deformed shape of the carcass may also lead to the “heart” mode. This is because the snap-through can only occur at a single point if the cross section is not in a perfect symmetrical shape. Once the snap-through takes place, the release of strain energy will stabilize any other possible failure points of the carcass immediately. This may explain why the “heart” mode is a typical mode shape that usually found in wet collapse tests (Paumier et al., 2009).

In addition, the deformed cross-sectional shape of the carcass can be influenced by the stiffness ratio of pressure armor to carcass (Malta et al., 2012). Actually, the deformed shape of the carcass at the collapse moment depends on the curvature level, symmetry condition of the initial ovalization as well as the stiffness of the pressure armor. Although the influence of the stiffness of pressure armor is not included in this work, further relevant studies should be carried out.

5. Conclusions

Following our previous mechanism study, an analytical model is established in this paper for predicting the wet collapse pressure of curved flexible risers. This analytical model is developed from a spring-supported arch model proposed in our previous work, which predicts the curved wet collapse pressure by incorporating the curvature-induced factors. The 3D full FE models presented in the mechanism study are employed to verify this analytical model. Based on the whole curved collapse studies, several conclusions can be drawn as follows:

(1) Both analytical and numerical studies reveal that the deformed cross-sectional shape of the carcass is the major contributing factor in curvature effect. For the models includes the pitch elongation and squeeze effect only, their results show that the pipe curvature could only trigger a slight decrease of the wet collapse pressure. Once the shape effect is introduced to those models, significant drop of the wet collapse pressure occurs with the increase of pipe curvature.
(2) The proposed analytical model has a good performance on predicting the wet collapse pressure of curved flexible pipes. This analytical model was used to predict the wet collapse pressure for a 4" ID flexible pipe with different curvature and initial ovalization types. By comparing analytical predictions to the numerical ones, the proposed analytical model is verified, in which the maximum error is 7.5%.
(3) This analytical model can be an efficient tool for the collapse analysis in pipe design stage. The numerical simulation in our case studies consumes 2∼3 days on average to finish one job. By contrast, the computational time required by the proposed analytical model takes only few seconds.

Up to now, the analytical models developed for curved collapse analysis of flexible pipes are very limited in public literature. Although numerical simulations can be an alternative, their high computational cost makes them less feasible for the collapse analysis in design stage. To fill this gap, an analytical model is presented in this work, which can take the curvature effect into account. The verification given by numerical simulation indicates that this analytical model can be a good choice for curved wet collapse issue.

CRediT authorship contribution statement

Xiao Li: Conceptualization, Methodology, Data curation, Verification, Writing - original draft. **Xiaoli Jiang:** Conceptualization, Writing - review & editing, Supervision. **Hans Hopman:** Supervision, Funding acquisition.

Declaration of competing interest

The authors declare that they have no known competing financial interests or personal relationships that could have appeared to influence the work reported in this paper.

Acknowledgment

This work was supported by the China Scholarship Council [grant number 201606950011].

References

API, 2014a. Recommended Practice for Flexible Pipe API RP 17B, fifth ed. American Petroleum Institute, Washington.
API, 2014b. Specification for Unbonded Flexible Pipe API Spec 17J, fourth ed. American Petroleum Institute, Washington.
Axelsson, G., Skjerve, H., 2014. Flexible riser carcass collapse analyses – sensitivity on radial gaps and bending. In: Proceedings of the 33rd International Conference on Ocean, Offshore and Arctic Engineering. American Society of Mechanical Engineers, San Francisco, California, USA, OMAE2014-23922.
Bai, Y., Yuan, S., Cheng, P., Han, P., Ruan, W., Tang, G., 2016. Confined collapse of unbonded multi-layer pipe subjected to external pressure. Compos. Struct. 158, 1–10.
Brazier, L.G., 1927. On the flexure of thin cylindrical shells and other "thin" sections. Proc. R. Soc. A 116, 104–114.
Brouard, Y., Seguin, B., Germanetto, F., Shah, V., 2016. Riser solutions for turret moored FPSO in Arctic conditions. In: Proc. 2016 Offshore Tech Conf. St John's, Newfoundland and Labrador, Canada. Paper No. OTC-27389-MS.
Caleyron, F., V., Le Corre, Paumier, L., 2017. Effect of installation on collapse performance of flexible pipes. In: Proceedings of the 36th International Conference on Ocean, Offshore and Arctic Engineering. American Society of Mechanical Engineers, Madrid, Spain, OMAE2017-61100.
Clarke, T., Jacques, R., Bisognin, A., Camerrini, C., Damasceno, S., Strohaecker, T., 2011. Monitoring the structural integrity of a flexible riser during a full-scale fatigue test. Eng. Struct. 33 (4), 1181–1186.
Clevelario, J., Pires, F., Falcão, G., Tan, Z., Sheldrake, T., 2010. Flexible pipe curved collapse behaviour assessment for ultra deepwater developments for the brazilian pre-salt area. In: Proc. 2010 Offshore Tech Conf. Houston, Texas, USA. Paper No. OTC-20636.
Crome, T., 2013. Experiences from design and operation, learning and improvements. Technip, PTiL Flexible Riser Seminar 2013.
Deng, K., Lin, Y., Liu, W., Zeng, D., Sun, Y., Li, K., 2016. Equations to calculate casing collapse strength under nonuniform load based on New ISO model. J. Press. Vessel Technol. 138, 054501.
Deng, K., Liu, B., Lin, Y., Sun, Y., Yuan, J., Tao, Z., 2019. Experimental study on the influence of axial length on collapse properties of N80 casing under non-uniform load. Thin-Walled Struct. 138, 137–142.
Gay Neto, A., Martins, C.A., 2012. A comparative wet collapse buckling study for the carcass layer of flexible pipes. J. Offshore Mech. Arctic. Eng. 134 (3), 031701.
Gay Neto, A., Martins, C.A., 2014. Flexible pipes: influence of the pressure armor in the wet collapse resistance. J. Offshore Mech. Arctic. Eng. 136 (3), 031401.
Gay Neto, A., Martins, C., Malta, E., Godinho, C., Neto, T., Lima, E., 2012. Wet and dry of straight and curved flexible pipes: a 3D FEM modeling. In: Proceedings of the 22nd International Ocean and Polar Engineering Conference, International Society of Offshore and Polar Engineers. ISOPE. Rhodes, Greece.
Glock, D., 1977. Überkritisches verhalten eines starr ummantelten kreisrohres bei wasserdruck von außen und temperaturdehnung (Post-critical behavior of a rigidly encased circular pipe subjected to external water pressure and thermal extension). Der Stahlbau 46, 212–217.
Gresnigt, A.M., 1986. Plastic design of buried steel pipelines in settlement areas. Heron 31 (4), 1–113.
Guarracino, F., 2003. On the analysis of cylindrical tubes under flexure: theoretical formulations, experimental data and finite element analyses. Thin-Walled Struct. 41, 127–147.
J.R.M., De Sousa, E.C.P., Lima, G.B., Ellwanger, A., Papaleo, 2001. Local mechanical behavior of flexible pipes subjected to installation loads. In: Proceedings of the 20th International Conference on Ocean, Offshore and Arctic Engineering. American Society of Mechanical Engineers, Rio de Janeiro, Brazil, OMAE2001/PIPE-4102.
Langhaar, H.L., 1962. Energy Methods in Applied Mechanics. Wiley, New York, USA.
Li, X., Jiang, X., Hopman, H., 2018a. A strain energy-based equivalent layer method for the prediction of critical collapse pressure of the flexible risers. Ocean Eng. 164, 248–255.
Li, X., Jiang, X., Hopman, H., 2018b. A review on predicting critical collapse pressure of flexible risers for ultra-deep oil and gas production. Appl. Ocean Res. 80, 1–10.
Li, X., Jiang, X., Hopman, H., 2020a. Curvature effect on wet collapse behaviors of flexible risers subjected to hydro-static pressure. Ships Offshore Struct. 1861705.
Li, X., Jiang, X., Hopman, H., 2020b. Predicting the wet collapse pressure for flexible risers with initial ovalization and gap: an analytical solution. Mar. Struct. 71, 102732.
Lin, Y., Deng, K., Sun, Y., Zeng, D., Xia, T., 2016. Through-wall yield collapse pressure of casing based on unified strength theory. Petrol. Explor. Dev. 43 (3), 506–513.
Loureiro, Jr., W.C., Pasqualino, I., 2012. Numerical-analytical prediction of the collapse pipes under bending and external pressure. In: Proceedings of the 31st International Conference on Ocean, Offshore and Arctic Engineering. American Society of Mechanical Engineers, Rio de Janeiro, Brazil, OMAE2012-83476.
Lu, J., Ma, F., Tan, Z., Sheldrake, T., 2008. Bent collapse of an unbonded rough bore flexible pipe. In: Proceedings of the 27th International Conference on Ocean, Offshore and Arctic Engineering. American Society of Mechanical Engineers, Estoril, Portugal, OMAE2008-57063.
Lukassen, T.V., Gunnarsson, E., Krenk, S., Glejbøl, K., Lyckegaard, A., Berggreen, C., 2019. Tension-bending analysis of flexible pipe by a repeated unit cell finite element model. Mar. Struct. 64, 401–420.
Mahé, A., 2015. Flexible pipe technology for deepwater and gas riser systems. In: GE Wellstream, AOG Perth Conference 2015.
Malta, E.R., Martins, C.A., Gay Neto, A., Toni, F.G., 2012. An investigation about the shape of the collapse mode of flexible pipes. In: Proceedings of the 22nd International Offshore and Polar Engineering Conference. ISOPE. Rhodes, Greece.

Martins, C.A., Pesce, C.P., Aranha, JAP., 2003. Structrual behavior of flexible pipe carcass during launching. In: Proceedings of the 22nd International Conference on Ocean, Offshore and Arctic Engineering. American Society of Mechanical Engineers, Cancun, Mexico, OMAE2003-37053.

Miyazaki, M., Paumier, L., Caleyron, F., 2018. Effect of tension on collapse performance of flexible pipes. In: Proceedings of the 37th International Conference on Ocean, Offshore and Arctic Engineering. American Society of Mechanical Engineers, Madrid, Spain, OMAE2018-77286.

Murawski, S.A, Hollander, D.J., Gilbert, S., Gracia, A., 2020. Deepwater oil and gas production in the gulf of Mexico and related global trends. In: Murawski, S., et al. (Eds.), Scenarios and Responses to Future Deep Oil Spills. Springer, Cham.

Paumier, L., Averbuch, D., Felix-Henry, L., 2009. Flexible pipe curved collapse resistance calculation. In: Proceedings of the 28th International Conference on Ocean, Offshore and Arctic Engineering. American Society of Mechanical Engineers, Honolulu, Hawaii, USA, OMAE2009-79117.

Rahmati, M.T., Bahai, H., Alfano, G., 2016. An accurate and computationally efficient small-scale nonlinear FEA of flexible risers. Ocean Eng. 121, 382–391.

Sævik, S., Ye, N., 2016. Aspects of Design and Analysis of Offshore Pipelines and Flexibles. Southwest Jiangtong University Press, Chengdu, China.

Simpson, P.J., Lima, A.J., 2019. Deepwater riser systems – historical review and future projections. In: Proc. 2019 Offshore Tech Conf. Rio de Janeiro, Brazil. Paper No. OTC-29787-MS.

Skjerve, H., Kristensen, C., Muren, J., Søfferud, M., Engelbreth, K.I., 2014. Findings from dissection and testing of used flexible risers. In: Proceedings of the 33rd International Conference on Ocean, Offshore and Arctic Engineering. American Society of Mechanical Engineers, San Francisco, California, USA, OMAE2014-24154.

Timoshenko, S.P., Gere, J., 1963. Theory of Elastic Stability. McGraw-Hill, New York, USA.

Tong, G., 2005. In-Plane Stability of Steel Structures. China Architecture & Building Press, Beijing.

Weppenaar, N., Andersen, B., 2014. Investigation of tensile armor wire breaks in flexible risers and a method for detection. In: Proceedings of the 33rd International Conference on Ocean, Offshore and Arctic Engineering. American Society of Mechanical Engineers, San Francisco, California, USA, OMAE2014-23103.